The Effect of Dielectric Barrier Discharge Plasma Actuators on Electromagnetics

F. Mirhosseini, *member, IEEE*, B. Colpitts, *Senior, IEEE* and R. Pimentel, Y. de Villers, *member, IEEE*

***Abstract*- Dielectric Barrier Discharge (DBD) plasma actuators have become very popular during the last decade. In aerodynamics, they have been employed for drag reduction, stability improvement, turbulence control, etc. In this paper the Radar Cross Section (RCS) of a plasma slab and moreover an extra reflection from plasma actuators because of Bragg diffraction are investigated. It was observed that plasma actuators operating in lower altitude conditions produce plasma with a very high collision rate and low electron density. Under these conditions, the dielectric properties of the plasma are not discernable from the air. As a result, at high pressure, the actuator has no significant effect on RCS. In contrast, for higher altitudes the air pressure decreases so electron life time increases and collision rate reduces, so the effect of plasma on incident electromagnetic wave can be observed. Additionally, the use of conventional plasma actuators being used in aerodynamics make more reflections at specific incident angles because of Bragg diffraction. This angle depends on the frequency and the spatial period of the actuator.**

***Index Terms*- Electro-hydrodynamics, dielectric barrier discharge actuator, Bragg Diffraction, radar cross section**.

I. INTRODUCTION

Potential benefits of electro-hydrodynamic (EHD) devices are very large and span from several applications, which has prompted significant interest and investment worldwide [1]-[4]. Nevertheless, because of the complexity of the physical phenomena involved most research is limited to controlled laboratory environments while focusing on the understanding of key parameters affecting performance of those devices. There remain several issues to be overcome before the technology could be integrated into practical applications [5], [6]. For instance, the effects of operating conditions on DBD actuator performance, electrical power requirements and suitability to high-speed regimes, in case of aeronautical and aerospace, are some of parameters that shall be addressed before using such devices into practical systems [7], [8].

Associated with the enhancements expected from the use of plasma in terms of aerodynamic performance there will also be changes in the radar cross section (RCS) performance of the vehicle [9]. These RCS changes may take the form of reduced cross section through plasma absorption or increased cross section through a change in the electrical shape of the target or the creation of a plasma plume [10].

RCS is defined as an effective area intercepting an amount of incident power and if the reflected power is scattered isotropically, it produces the same level of power at the radar equal to that from the target. Thus the scattering ability of a target is expressed in units of area, normally square meters. This scattering cross section is highly dependent upon the target shape materials and viewing angle [9]. In this paper we investigate the effect of plasma slab on the RCS of a conductive sheet. The RCS is simulated and measured to verify the validity of the model used for simulations. Moreover, we show the DBD actuator generates an extra reflection because of Bragg diffraction while this phenomenon is not noticed by now in the literature.

II. RCS Simulations from conductive flat plate and DBD actuators

In order to simulate and measure the effect of plasma slab on the RCS change of a conductive layer, an experimental setup was used as shown in Fig. 1. This structure allows the generation of plasma that stands by itself in the tube. A conductive layer is installed the other side of the tube and is used to reflect the RF signal back to the tube. Plasma is generated in a cylindrical glass tube in which pressure can be controlled. The outer diameter of the tube is 51 mm and the inner diameter is 47 mm. Copper tape of width 25 mm and length 100 mm is used as electrodes on the glass tube. A (0.96 - 1.45 GHz) WR770 waveguide with aperture dimensions of 196 mm×98 mm is used as the transmitting and receiving antenna to generate a RF signal polarized perpendicular to the electrode length. The distance between the waveguide and the glass tube is 70 mm and between the conductive layer and tube is 120 mm. Using this structure, a plasma region can be generated in order to measure its effectiveness for the RCS suppression. The same experiment was repeated by a WR90 waveguide for x-band (9-11 GHz).

A. Validation of Modelling

Fig. 2 shows the comparison between simulation and measured values of the coefficient of reflection (S11) difference for a plasma layer of thickness 25 mm corresponding to the electrode width, while the thickness of DBD actuator plasma is 2.5 mm [6]. First, the RCS of copper plate is simulated and measured when plasma is off. Then, the plasma turns on and the simulations and measurements are done for two different pressures (15 torr and 35 torr). The S11 for both pressures is achieved when plasma is off and on. The values of S11 for the case with no plasma are subtracted from the ones with plasma layer on, so the S11 differences for both gas pressures are achieved. The plasma parameters used for simulations are based on values in table I [11].

Table I
Plasma parameters for two different pressures [11]

Elevation (m)	Pressure (Torr)	Collision Rate (υ) GHz	Electron Density (n_e) $10^{14}/m^3$	Plasma Frequency (f_p) MHz
27490	15	0.92	6.28	226
21554	35	1.46	2.69	148

The applied voltage was 10 kV (peak-to-peak) with a frequency of 5 kHz. By setting up these parameters, plasma with electron density of $n_e = 6.28 \times 10^{14}\ /m^3$ will be generated for 15 torr, and $n_e = 2.69 \times 10^{14}\ /m^3$ for 35 torr. In other words, the S11 difference between the two cases, when the conductive sheet is not covered by a plasma layer and when it is covered by plasma is simulated and measured. A reduction of 0.5 dB in reflected power from the conductive layer is produced for frequencies around 1.5 GHz revealed in Fig. 2(a). Maximum RCS reduction is predicted to occur for frequencies close to the electron-neutral collision rate which is 1.46 GHz at the pressure of 35 torr atmosphere which is confirmed in both the measured and simulated results shown and compatible with plasma physics predictions [12]. The differences between measured and simulated S11 curves are due to reflections in the experimental setup which are not present in the more ideal simulations. In Fig. 2(b) the S11 difference for both cases is measured and simulated for 10 GHz. As it can be seen the reflection power reduction is less than that for the case with f=1.5 GHz, as predicted by theoretical plasma physics. By increasing the incident wave frequency the plasma gets more transparent and so the attenuation decrease.

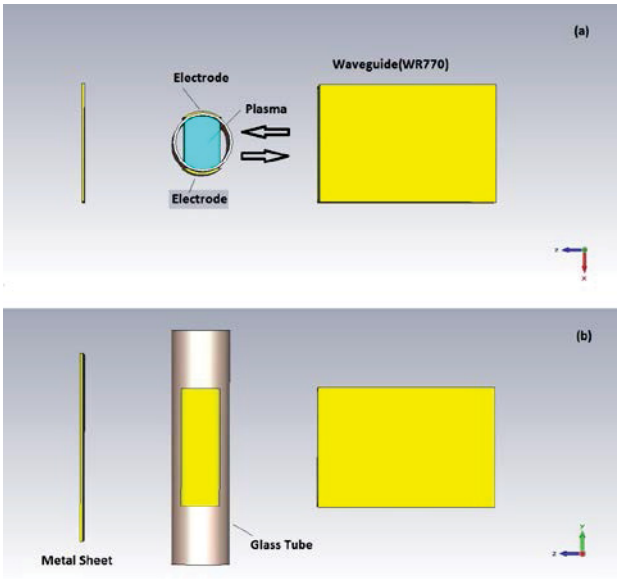

Fig. 1. The experimental set up used for measuring the influence of plasma on RCS. (a) Top view. (b) Side view.

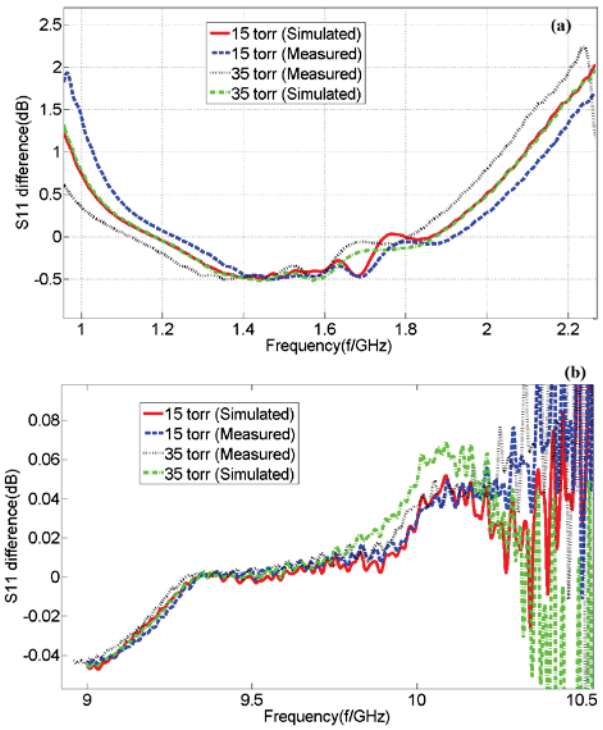

Fig. 2. S11 difference between a conductive plate with the plasma region present compared to the case of no plasma. The glass tube remains in place in both cases. Absorption by the plasma is small for both simulated and measured results showing good agreement over the frequency range. (a) S11 difference using WR770. (b) S11 difference using WR90.

For this measurement, the power source is synchronized with the Voltage Network Analyzer (VNA), so the reflection parameter (S11) is measured at maximum electron density when the applied voltage is at peak. To do this, a visual basic code was written using predefined VNA objects and VNA is calibrated. This enables automatic measurements on a specific number of frequency points for a specified frequency band.

The RCS can be reduced theoretically using plasma installed at specific locations on a target but it is very difficult or even impossible to create such a scenario in a realistic setting. In particular at high atmospheric pressure, the electrons density is sufficient high that collisions in the plasma occur at very high rates making the generation of plasma challenging and RCS reduction more difficult. We show through numerical modelling and experiment that there are measureable effects of plasma under high altitude conditions but these correspond to altitudes beyond conventional aircraft [11], for example, 15 torr corresponds to an altitude of 27 Km.

It is possible to design theoretical plasma capable of providing RCS reduction. If one can arbitrarily select the plasma collision rate and electron density and profile as well as the thickness then it can be made to absorb radar signals. This has been shown in [12]-[15]. However, practical or even laboratory implementation of these scenarios seems difficult. The collision rate is determined by the atmospheric pressure and electron temperature and density, and at normal

atmospheric pressure, the recombination rates are too high for significant absorption to occur [16]. In addition to this, the need to generate plasma throughout a volume and preferably change the plasma properties with position. Potential generation methods might include high power microwaves, or high power lasers. In either case, the energy requirements will be large producing an even more troublesome situation than without using plasma. That is, instead of reducing the visibility of the target one is now turning it into a powerful microwave or infrared beacon which would be easily detected. The DBD actuator, investigated in subsection B, shows that it can appreciably affect RCS.

B. DBD Actuators

Plasma generated by DBD actuators has nearly the same characteristics as air from the point of view of the incoming radar signal, that is, the relative permittivity is close to one because of the high collision rate at atmospheric pressure [16]. This is further constrained by the very spatially thin layer of plasma produced by the actuator, which is about 2 mm [6]. At lower pressures, corresponding to very high altitudes, the collision rates are low enough that the plasma will have electrical characteristics different than the surrounding air and there will be an opportunity for RCS reduction. Again the very thin nature of the actuator plasma could limit this effect.

Fig. 3 shows the structure used for simulation and measurements. The dimension of the copper and dielectric base is 30×40 cm. The dielectric is then covered by 10 DBD actuators formed from copper stripes with dimension of (20 mm×300 mm) separated by (15 mm×300 mm) gaps. The copper tape has a thickness of 0.2 mm.

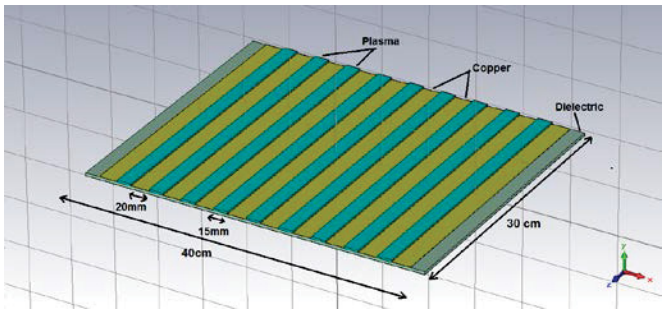

Fig. 3. DBD actuator structure used for simulations and measurements.

A plasma layer with a thickness of 2 mm covers the gap between copper stripes. For air pressure of 15 torr, 10 kV peak-to-peak voltage and a frequency of 5 kHz, a plasma frequency and collision rate of $\omega_p = 1.42\,Grad/s$ and $\upsilon = 1\,GHz$ can be obtained. For the simulations, a commercial software (CST-MWS) is used.

Fig. 4 shows the monostatic electric field of the DBD actuator at 10 GHz when the incident wave is vertically polarized or the E field is in +z direction. θ and φ are angles with respect to the z and x axis. This simulation shows the the reflected electric field increases for both field components (E_θ and E_φ) in the presence of the plasma.

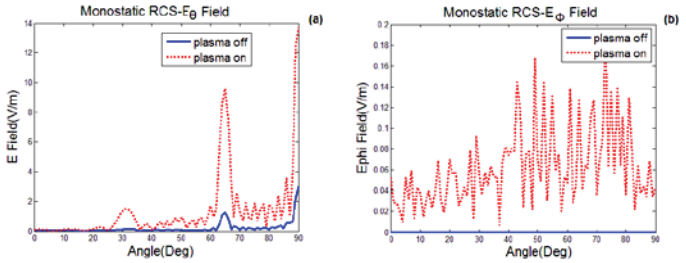

Fig. 4. Monostatic Electric field of DBD actuator with 10 elements at 10 GHz for vertically polarized incident wave. (a) E_θ (b) E_φ.

Fig. 5 shows the monostatic electric field of the same structure of Fig. 3 for incident E-field polarized along the stripes or horizontal polarization. In other words, electric field of incident wave has no zero component in (+z) direction and φ varies from 0^o to 180^o. These results show the increased RCS induced by the plasma for the actuator presented in Fig. 3.

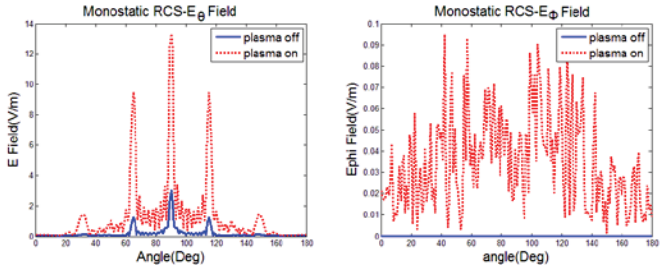

Fig. 5. Monostatic Electric field of DBD actuator with 10 elements at 10 GHz for horizontally polarized wave. (a) E_θ (b) E_φ.

Fig. 6 shows the RCS of DBD actuator for 10 GHz when plasma is off and when the plasma is on. It can be seen the RCS will increase plasma is on.

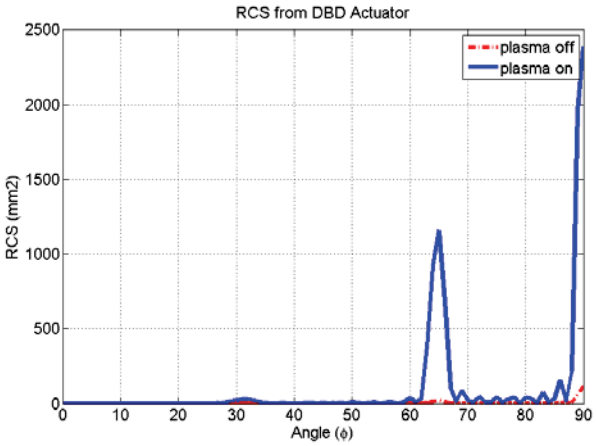

Fig. 6. Comparing the RCS of DBD actuator when plasma is on and off

C. Bragg diffraction from DBD plasma actuator

Plasma actuators are used on aircraft for drag reduction or propulsion improvement. There is a significant body of literature describing and optimizing actuators for the highest performance as mentioned in section I. As we have shown at high pressure the actuators do not have any significant effect on RCS while at lower pressures the plasma layer can slightly lower RCS. An important factor which is ignored in the previous research is that for some angles actuators may even increase RCS due to Bragg diffraction.

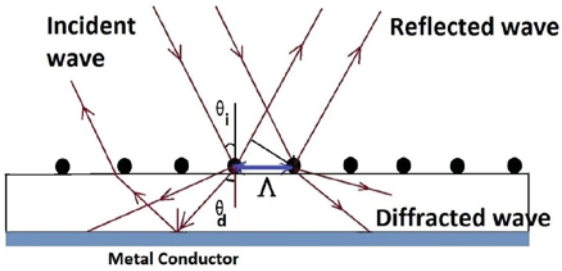

Fig. 7. Diffraction from a periodic structure.

Coherent illumination of an array of dielectric or conductive gratings will result in directional scattering of the incident wave. When electromagnetic waves are scattered from a crystal lattice or grating, peaks of scattered intensity are observed when the path length difference is equal to an integer number of wavelengths.

The condition for maximum intensity of bi-static RCS occurs for a specific diffraction angle as defined in (1).

$$\sin\theta_d - \sin\theta_i = m\frac{\lambda/n}{\Lambda} \tag{1}$$

Where λ is the wavelength of incident wave, Λ is the distance between two array elements, and θ_i and θ_d are the incidence and diffraction angles. For the plasma actuators discussed in this paper, the conductor strips act as crystal units. In this case, the grating diffraction reduces to the Bragg diffraction and (1) changes to (2) [17].

$$2\Lambda\sin\theta_d = m\frac{\lambda}{n} \tag{2}$$

For the simulations, two different actuators were used. For the first one, the following parameters were used ($\Lambda = 80$ mm, w $= 35$ mm, f $= 5.8$ GHz) and for the second one, the following parameters were used($\Lambda = 35$ mm, w $= 20$ mm, f $= 8$ GHz). Fig. 8(a) shows the result of simulations for backscattered wave in terms of electric field. To find the Bragg diffraction angle, the simulation software Computer Simulation Technology-MicroWave Studio (CST-MWS) was used. A plane wave with z-polarization is simulated using different parametric variables so it scans the incidence angles from 0^o to 90^o in one degree steps. Two different radar frequencies were used for these simulations (5 and 8 GHz). Figure 8(a) presents two peaks at 71 degree (red curves) and 58 degree (blue curve) which corresponds to the reflection angle resulting from the Bragg diffraction phenomena. This corresponds to the diffraction angles 19^o and 32^o respectively. This is in good agreement with calculations using equation (2) which results in $\theta_d = 18.86^o$ and $\theta_d = 31.85^o$.

Fig. 8.b shows the measured S11 from a 6-element plasma actuator at 8GHz. The width of the copper strips is 2cm and a gap between two strips is 1.5cm. Three peaks can be observed on this figure. The biggest one is associated to the specular reflection which happens at 90^o and the two other peaks occur, one at 58^o and the other at 122^o. These two peaks occur because of Bragg diffraction which for 8GHz happens at 58 degree (32 degree from 90^o) using (2), so there is a good agreement between theory and experiment

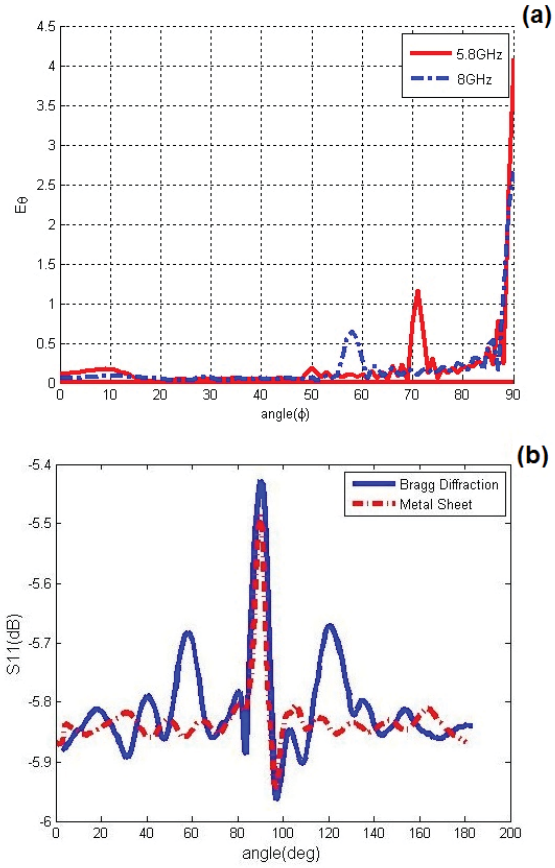

Fig. 8. (a) Mono-static reflection of wave from actuators showing the angles of maximum backscattered electric field. (b) The measured mono-static reflection from plasma actuator at 8 GHz.

III. Conclusion

Plasma actuators operating in the lower altitudes produce plasma with a very high collision rate and low electron density. Under these conditions, the dielectric properties of the plasma are not discernable from the air with our very sensitive experimental procedure. As a result, at high pressure, the actuator has no significant effect on RCS. In contrast, for higher altitudes the air pressure decreases so electron life time increases and collision rate reduces, so the effect of plasma on incident electromagnetic wave can be observed. Moreover,

using conventional plasma actuators make more reflections at specific incident angles because of Bragg diffraction. This angle depends on frequency and the spatial period of the actuator.

References

[1] L. H. Feng, T. N. Jukes, K. W. Choi and J. J. Wang, "Flow control over NACA 0012 airfoil using dielectric-barrier-discharge plasma actuator with a gurney flap," *Exp. Fluids,* Vol. **52, No. 6,** pp. 1533-1546, Jun. 2012.

[2] R. Pereira, D. Ragni and M. Kotsonis "Effect of external flow velocity on momentum transfer of dielectric barrier discharge plasma actuators," *J. Appl. Phys*., Vol. 116, No. 10, Sep. 2014.

[3] X. Li, W. Bao and C. Di "A brush-shaped air plasma jet operated in glow discharge mode at atmospheric pressure," *J. of Appl. Phys*., Vol. 116, No. 2, Jul. 2014.

[4] H. Otsu, Y. Kamada, Y. Yamagiwa and T. Ohno, "Attitude Control of UAV using DBD plasma actuator," *27th international congress of the aeronautical sciences,* 2010.

[5] E. Moreau, R. Sosa**,** and G. Artana, "Electric wind produced by surface plasma actuators: a new dielectric barrier discharge based on a three-electrode geometry," *J. Phys. D: Appl. Phys.*, Vol. 41, No. 11, May 2008.

[6] H. Nishida, T. Nonomura and T. Abe, "Three-dimensional simulations of discharge plasma evolution on a dielectric barrier," *Journal of Applied Physics,* Vol. 115, No. 13, Apr. 2014.

[7] Z. Chen, Z. Yin, L. Hong and G. Xia, "Self-consistent fluid modeling and simulation on a pulsed microwave atmospheric-pressure argon plasma jet," *J. Appl. Phys*., Vol. 116, No. 15, Oct. 2014.

[8] S. Wu, Z. Wang, Q. Huang, and X. Tan, "Atmospheric-pressure plasma jets: Effect of gas flow, active species, and snake-like bullet propagation," *Physics of Plasmas*, Vol. 20, No. 2, Feb. 2013.

[9] W. Q. Wang**, "**Radar Systems: Technology, Principles, and Applications," New York: Nova Science Publishers, Inc., 2013.

[10] M. Keidar, D. Boyd, E. Antonsen, and G. G. Spanjers, "Electromagnetic effects in the near-field plume exhaust of a micro-pulsed-plasma thruster," *J. of Propulsion and Power*, Vol. 20, No. 6, pp.961-969, Dec. 2004.

[11] F. Mirhosseini and B. Colpitts, "Plasma actuator electron density measurement using microwave perturbation method," *Appl. Phys. Lett.* Vol. 105, No**.** 5, July 2014.

[12] S. S. M. Chung, "FDTD simulations on radar cross sections of metal cone and plasma covered metal cone," *Vacuum,* Vol. 86, No. 7, Feb. 2012.

[13] H. W. Yang and Y., "SO-FDTD Analysis on the Stealth Effect of Magnetized Plasma with Epstein Distribution," *Optik,* Vol. 124, No**.** 15, Aug. 2013.

[14] Z. Han, J. Ding , P. Chen, Z. Zhang and C. Guo, "FDTD analysis of three-dimensional target covered with inhomogeneous un-magnetized plasma," *International Conference on Microwave and Millimeter Wave Technology*, ICMMT, 2010.

[15] S. Zhang, X. Hu, Z. Jiang, M. Liu and Y. He "Propagation of an electromagnetic wave in an atmospheric pressure plasma: Numerical solutions," *PHYSICS OF PLASMAS,* Vol. 13, No. 1, Jan. 2006.

[16] P. M. Bellan, "*Fundamentals of Plasma Physics*," Cambridge University Press, Cambridge, 2008.

[17] M. Born and E. Wolf, "Principles of Optics: electromagnetic theory of propagation, interference and diffraction of light," Cambridge, New York: Cambridge University Press, 1999.

Farid Mirhosseini (M'12) was born in Mashhad, Iran. He received the B.Sc.E., M.Sc.E., degrees in electrical engineering in 1998 and 2001 respectively from Tehran Polytechnic and Ferdowsi University of Mashhad, Iran. During his master, he worked on integrated optics including relief surface diffraction gratings and multilayer optical filters. He is now working on his Ph.D. at University of New Brunswick, Fredericton, NB, Canada. For his Ph.D. research, he has worked on plasma radar cross section. His research interests are primarily related to computational and theoretical electromagnetics, electromagnetic inverse scattering, RF/microwave and millimeter wave systems, microwave photonics, antennas (phased array, UWB and microstrip), and integrated optics; including design, simulation, measurement, hardware fabrication and development, and application. Recent projects include the Plasma characteristics measurement using cavity perturbation method, plasma radar cross section, simulation and modelling of electromagnetic wave interaction with dispersive media.

Dr. Bruce G. Colpitts received the B.Sc.E., M.Sc.E., and Ph.D. degrees in electrical engineering in 1983, 1985, and 1988, respectively, from the University of New Brunswick, Fredericton, NB, Canada where he is currently Professor. His research interests are primarily related to microwave systems, antennas, and propagation; including measurement, simulation, hardware development, and application. Recent projects include the development of a portable harmonic radar tracking system, the development of a microwave reflectometer instrument, ongoing development of fibre optic based strain and temperature sensing instruments, RF and magnet design for improved MRI, and numerous antenna designs.

Rogerio Pimentel was born in Rio de Janeiro, Brazil. He received his M.Sc. and Ph.D. degrees in mechanical engineering from Université Laval on the development of numerical and experimental strategies for liquid

fuel atomization and injection applied to pulse detonation engines. He joined Defense Research and Development Canada as defense scientist in 2005 and he has been responsible for the DRDC tri-sonic wind tunnel and ballistic laboratory facilities. He is adjunct professor at Université Laval since 2007. He has been involved in studies of enabling technologies for high-speed vehicles in the field of combustion and flight mechanics. His research interests include high-speed propulsion and aerodynamics and thermal, flash and recoil management of small arms.

Yves de Villers (M'80) was born in 1956 in Quebec City, Canada. He received his B. Sc. Ap., and M. Sc. Ap. from Université Laval in 1980 and 1984, in electrical engineering. From 1982, he has been a defense scientist at the Defense Research Establishment, Valcartier. He has being involved in research and development of millimeter wave systems and signal processing systems. His research interests include millimeter-wave system, infrared imaging system, DSP and FPGA real-time signal processing. ATR and ATC technique including artificial neural networks. He is member of IEEE Quebec section executive since 1984 as chairman, treasurer and membership development officer. He was also chairman of the Quebec chapter of AES (2004-103). He is now active as secretary of the Quebec section.